Supplementary information to accompany: Simultaneous Observation of Kinesin-Driven Microtubule Motility and Binding of Adenosine Triphosphate Using Linear Zero-Mode Waveguides

*Ryuji Yokokawa

Department of Micro Engineering, Kyoto University

Kyoto Daigaku-Katsura, Nishikyo-ku, Kyoto 615-8540, Japan

Tel/Fax: +81-75-383-3682

Email: ryuji@me.kyoto-u.ac.jp

Contents

1. Supplementary figures

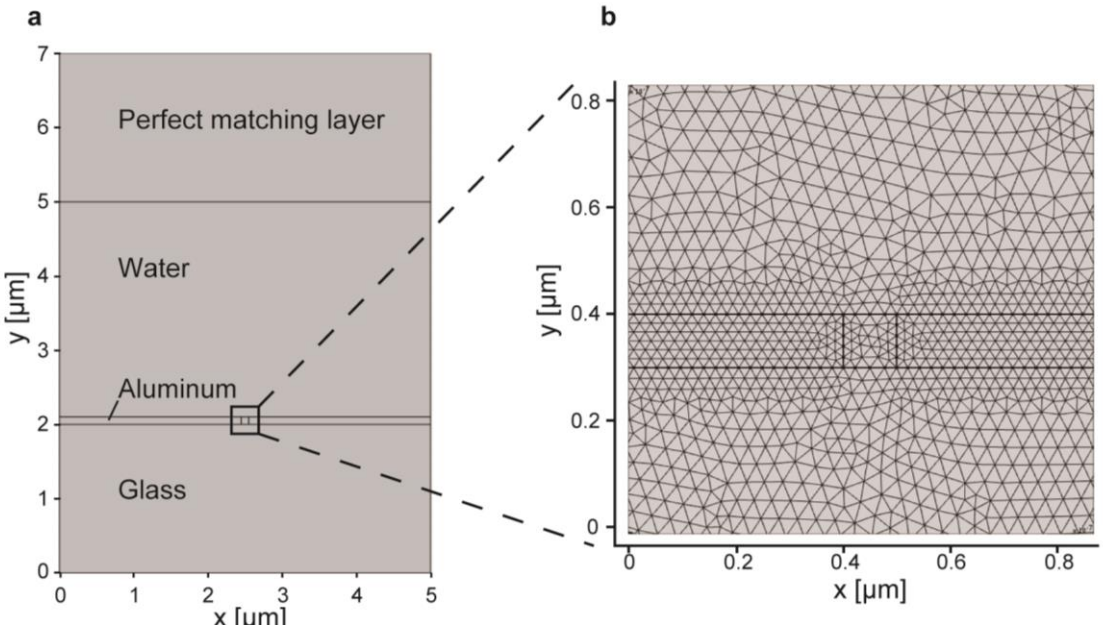

Supplementary Figure 1. The model used for COMSOL simulation. a) Definition of materials. b) Enlarged view of simulation mesh around the track structure.

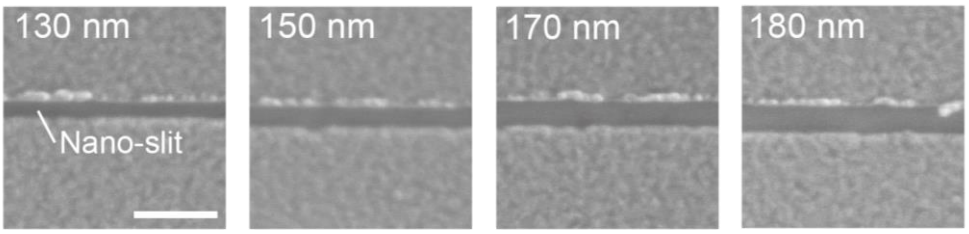

Designed width	Measured width
130 nm	108.4 ± 7.4 nm
150 nm	132.4 ± 8.2 nm
170 nm	154.8 ± 7.3 nm
180 nm	165.2 ± 8.2 nm

Supplementary Figure 2. Relationship between measured and designed nano-slit widths. Scale bar: 500 nm.

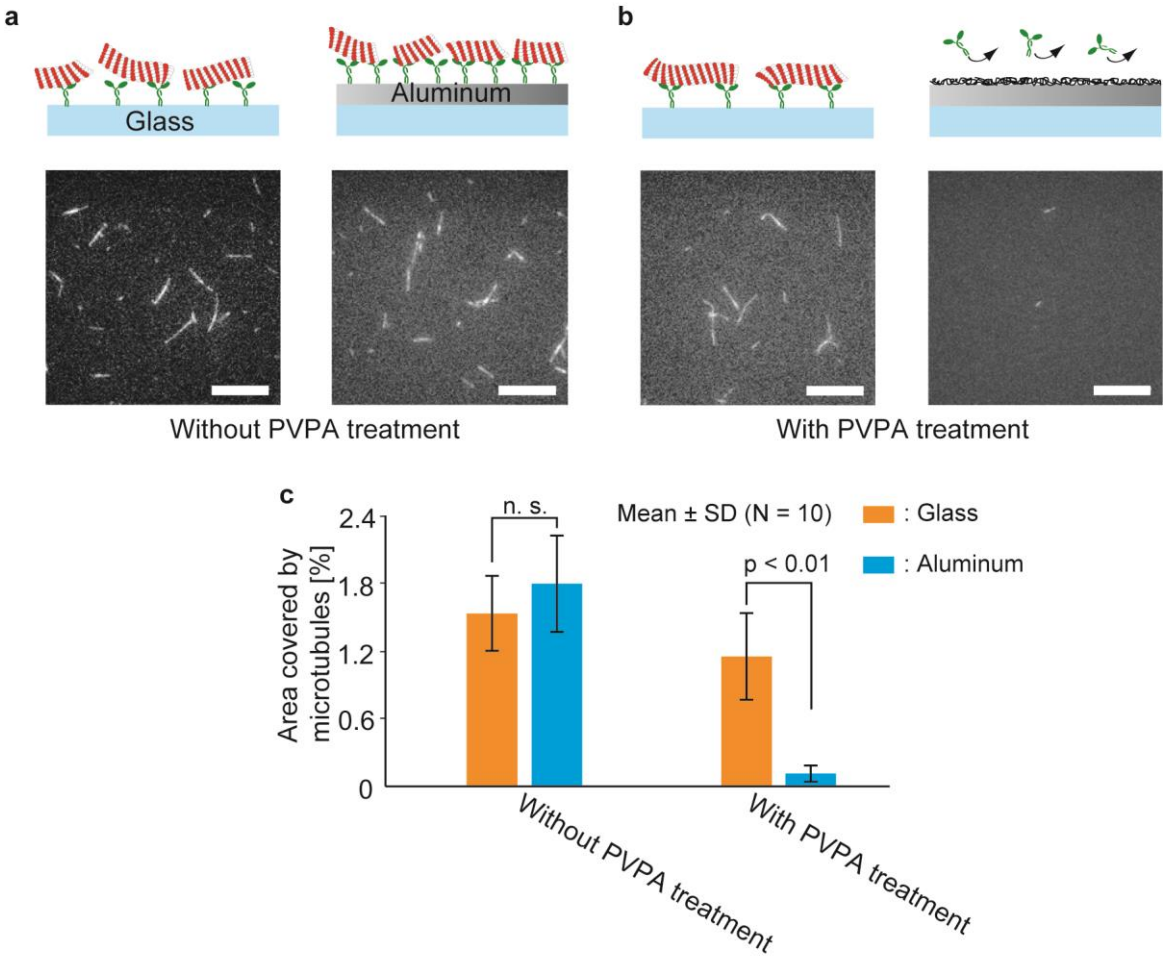

Supplementary Figure 3. Density of microtubules on aluminum and glass surfaces with or without PVPA treatment. a) Microtubules attached to the glass surface (left) and aluminum surface (right) without PVPA treatment. b) Microtubules attached to the glass surface (left) and aluminum surface (right) with PVPA treatment. c) Area covered by microtubules. With PVPA treatment, the area covered by the microtubules was significantly reduced on the aluminum surface. Scale bar: 10 μm.

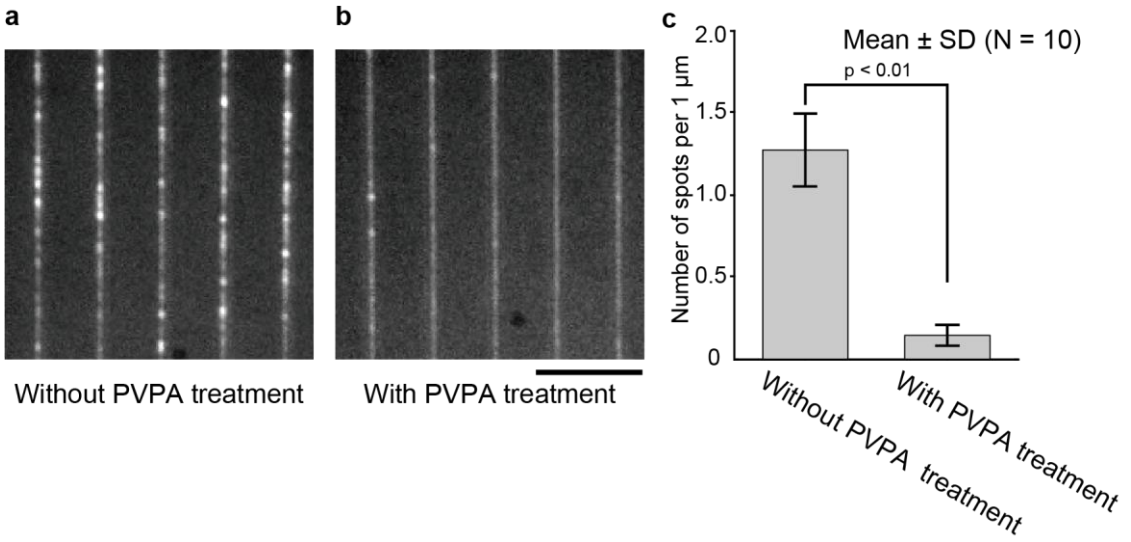

Supplementary Figure 4. Effects of PVPA treatment for nonspecific adsorption of labeled ATP. a) Many fluorescent spots were observed in non-PVPA treated LZMWs. b) In PVPA-treated LZMWs, nonspecific adsorption was suppressed. c) Number of ATP spots per 1-µm track. PVPA treatment significantly suppressed nonspecific adsorption of ATP in LZMWs. Scale bar: 2 µm.

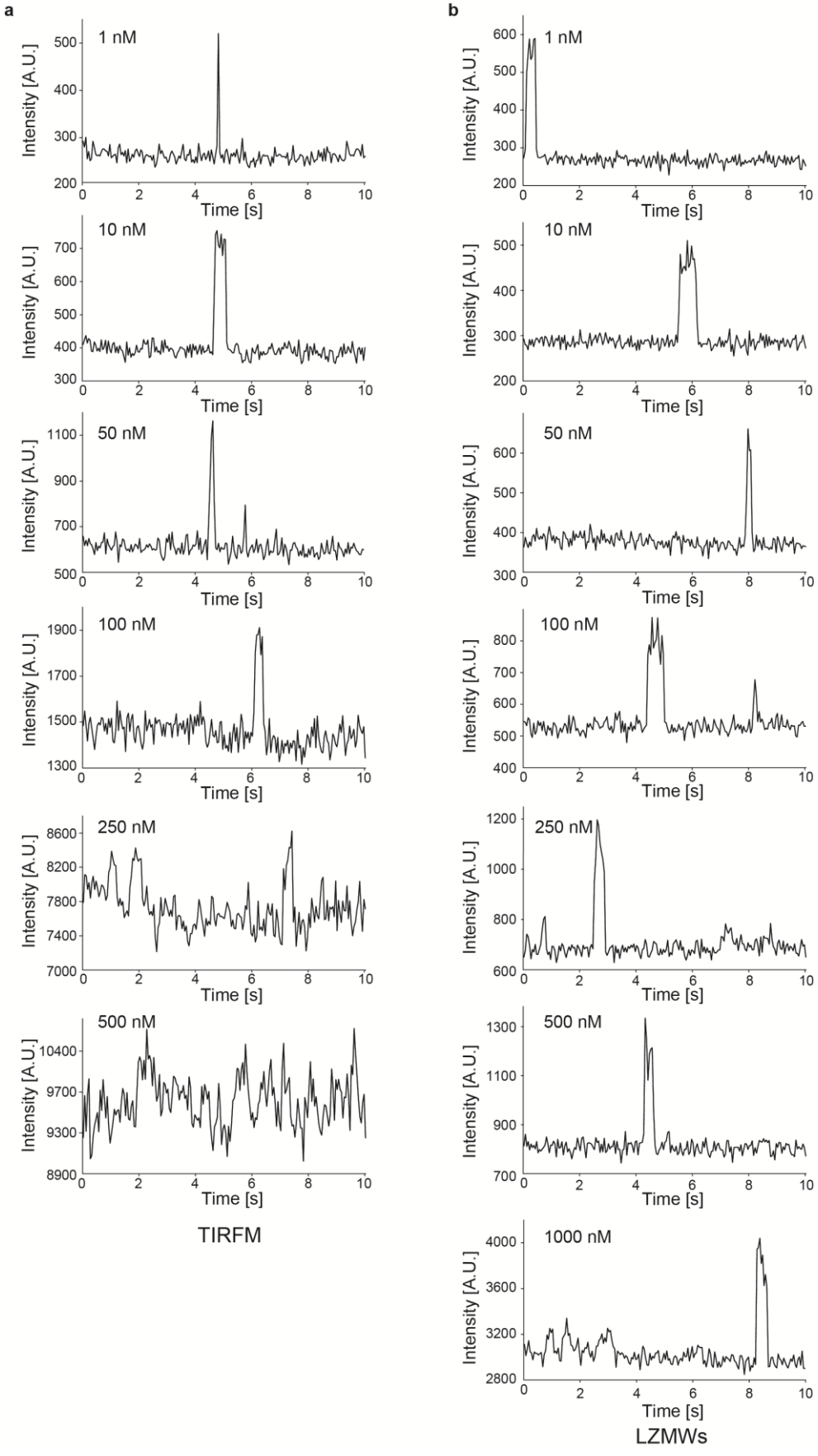
a
1 nM
10 nM
50 nM
100 nM
250 nM
500 nM
Intensity [A.U.]
Time [s]
TIRFM
b
1 nM
10 nM
50 nM
100 nM
250 nM
500 nM
1000 nM
Intensity [A.U.]
Time [s]
LZMWs

Supplementary Figure 5. Time traces of fluorescent intensities using a) TIRFM and b) LZMWs for 1–1000 nM labeled ATP.

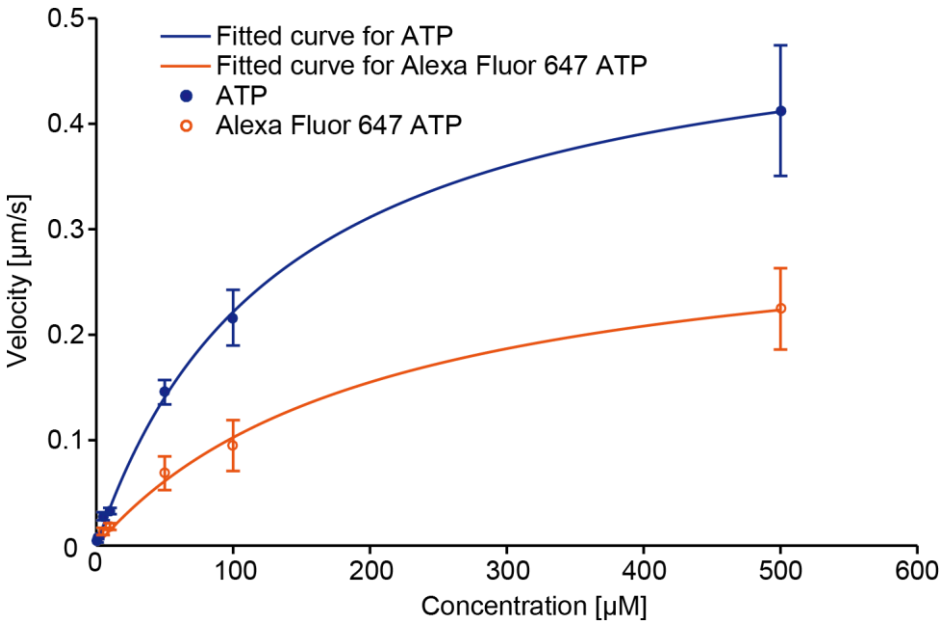

Supplementary Figure 6. Velocity of Qdot-kinesin with unlabeled ATP (blue closed circles) and Alexa Fluor 647-labeled ATP (orange open circles). Velocities were fitted with the Michaelis-Menten equation (blue and orange lines).

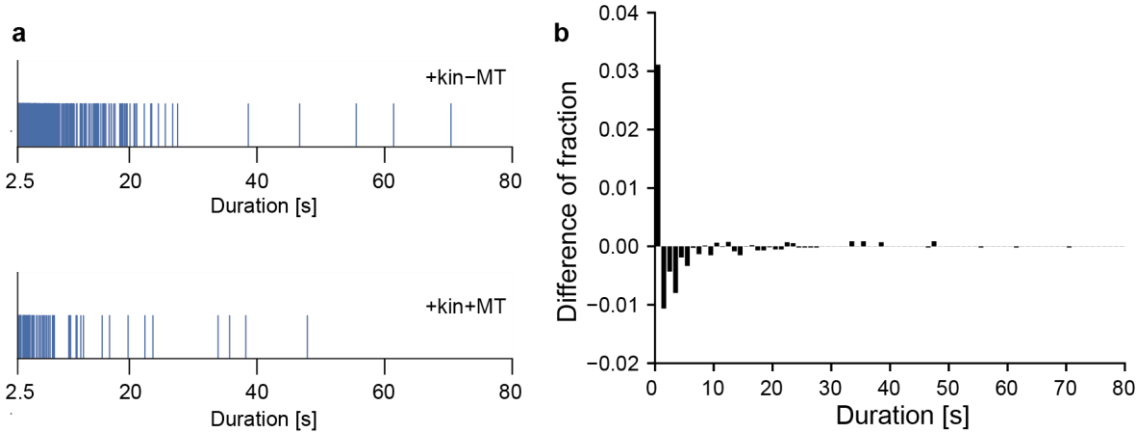

Supplementary Figure 7. ATP binding at longer duration. a) Distributions of ATP binding without microtubules (+kin − MT) and with microtubules (+kin+MT) at durations of > 2.5 s, which is out of the plot area in Fig. 4g. b) Difference in duration distributions between conditions with microtubules (+kin+MT) and without microtubules (+kin − MT) from 0 to 80 s.

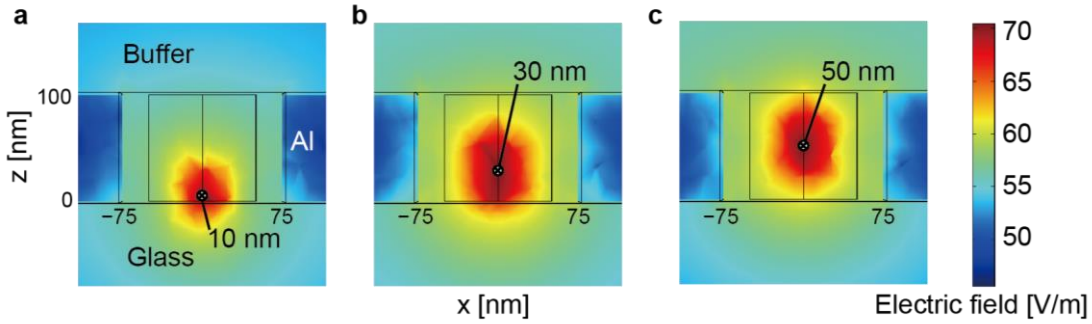

Supplementary Figure 8. Distribution of the electric field formed by radiation from a dipole in LZMWs. The distances from the glass surface to the dipole were a) 10 nm, b) 30 nm, and c) 50 nm.

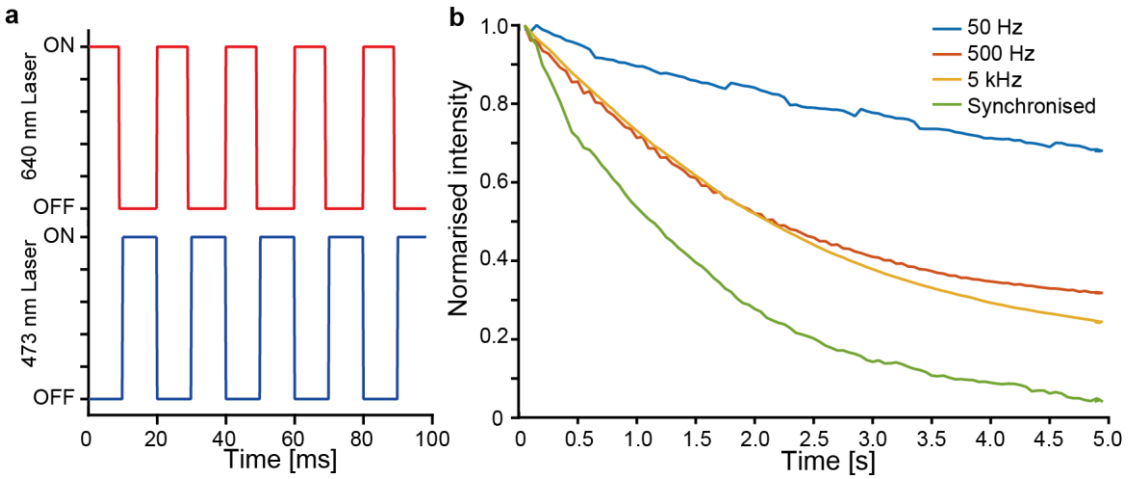

Supplementary Figure 9. Suppression of photobleaching by alternating excitation by 640 and 473 nm laser sources (Supplementary Movie 6). a) Schematic representation of control signals to alternately turn on and off two laser sources. The phase of the signal was shifted by 180°. b) Photobleaching of labeled ATP at 50 Hz, 500 Hz, and 5 kHz. "Synchronized" indicates photobleaching without a phase shift at 50 Hz.

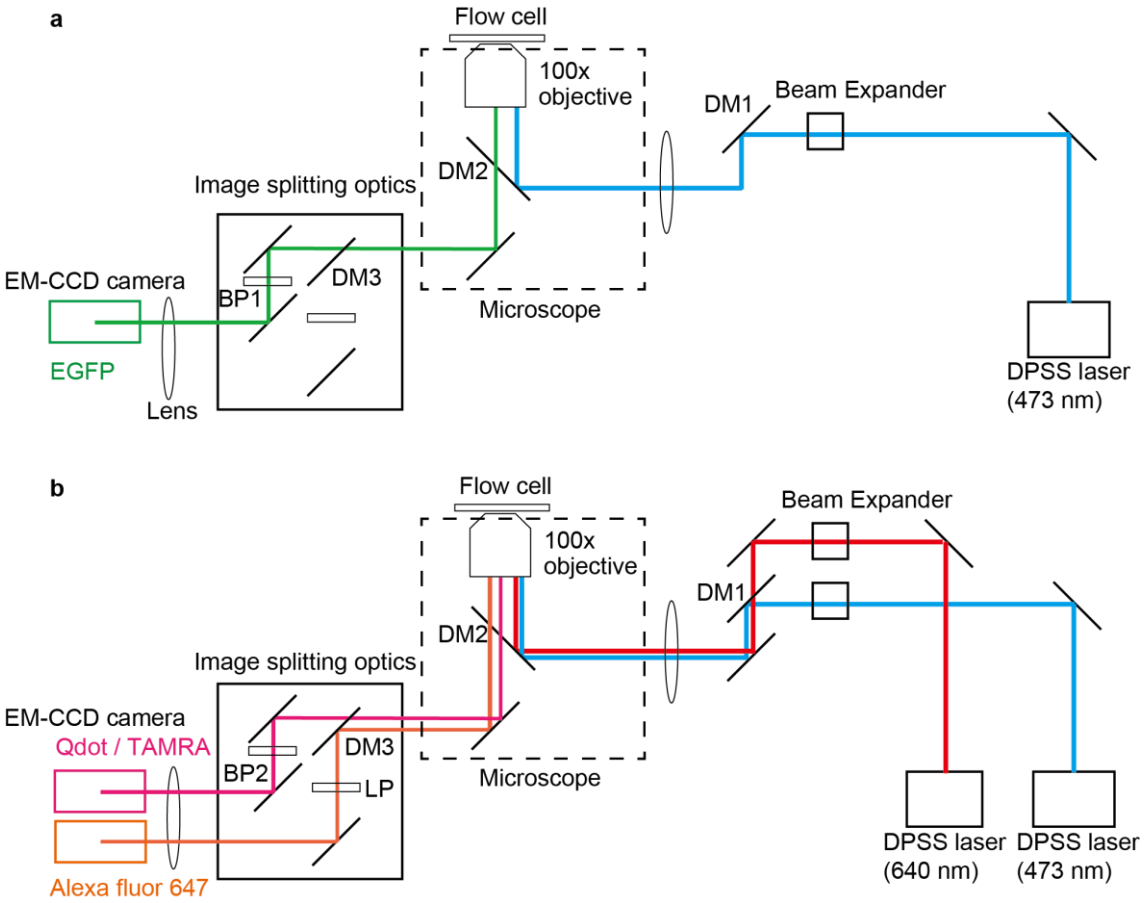

Supplementary Figure 10. Optical setup used for experiments. a) A 473-nm laser was used to excite EGFP. b) For simultaneous observation of Alexa Fluor 647 and Qdot 585, two diode laser sources were coupled to a 100× objective lens for TIRFM or epifluorescence modes. Fluorescent signals were projected to an EM-CCD camera after separation by W-view. DM: dichroic mirror, BP: bandpass filter; LP: longpass filter.

2. Supplementary Table

Supplementary Table 1. Functional properties of kinesin

	K_m [M]	V_{max}	k_{cat}[1]	k_{on}[2]
Labeled ATP	209 μM	316 nm s^{-1}	40 s^{-1}	1.9×10^5 $M^{-1}s^{-1}$
Unlabeled ATP	136 μM	532 nm s^{-1}	65 s^{-1}	4.8×10^5 $M^{-1}s^{-1}$

1. Values of k_{cat} were calculated by dividing the values of V_{max} by 8 nm.
2. Values of k_{on} were calculated by k_{cat}/K_m.

3. Supplementary Methods

Measurement of the signal-to-noise ratio

To evaluate changes in fluorescent intensities over time under various conditions, 3 × 3 pixels around the center of a single Alexa Fluor 647-labeled ATP were set as the region of interest. To distinguish noise from fluorescent signals of labeled ATP, we defined a threshold I_s as below,

$$I_s = I_{\mathrm{median}} + I_{\mathrm{SD}}, \tag{S1}$$

where I_{median} is the median, and I_{SD} is the standard deviation calculated from intensity values in all frames of the fluorescent image sequence. Intensities below and above I_s were classified as noise and signal, respectively. In addition, the signal value S was calculated as

$$S = S_{\mathrm{mean}} - N_{\mathrm{mean}}, \tag{S2}$$

where S_{mean} and N_{mean} were the average signal and noise values, respectively. The noise level N was calculated as the standard deviation of the noise value, and the S/N ratio was calculated as the ratio of S to N.

Effective observation volume inside LZMWs

The effective observation volume was calculated according to Levene *et al.* using the effective observation profile[1]. The profile was calculated as a function of the distance z from the bottom surface of LZMWs,

$$S(z) = I(z)p(z)Q(z) \quad , \tag{S3}$$

where $I(z)$ is the excitation intensity as a function of the distance from the bottom surface, $p(z)$ is the dipole coupling efficiency, and $Q(z)$ is the quantum yield function. $I(z)$ was calculated as exponential decay, which fits the simulated electric field intensities. Radiation from a dipole was calculated by FEM simulation with three dipole orientations (Supplementary Fig. 8). The dipole coupling efficiency was calculated as the ratio of the radiation energy reaching the objective lens to the whole radiation from a dipole. The efficiency decayed as the distance from the bottom of the slit increased. Therefore, the function $p(z)$ was obtained as exponential decay fitting of the efficiencies averaged for three dipole orientations with dipoles at various distances. $Q(z)$ was defined with $p(z)$,

$$Q(z) = \frac{p(z)}{p(z) + C} \quad , \tag{S4}$$

where constant C was set as 2.0, to match the boundary condition, $Q(0) = 0.33$, derived from the quantum yield of the Alexa Fluor 647 dye in bulk condition. The effective volume V_{eff} was given by

$$V_{\mathrm{eff}} = \quad W\delta \frac{(\int S(z))dz)^2}{\int S^2(z)dz} \quad , \tag{S5}$$

where W is the width of LZMWs, and δ is the diffraction limit. When the wavelength of the excitation light was 640 nm with a 100× objective lens (N.A. = 1.40), V_{eff} was calculated as 2.0×10^{-18} L (2.0 aL).

Calculation of the association rate constant

The ATP concentration-velocity curve was obtained from single-molecule motility experiments (Supplementary Fig. 6). To calculate the association rate constant, the curves were fitted with Michaelis-Menten kinetics,

$$V \equiv \frac{d[P]}{dt} = \frac{V_{\mathrm{max}}[S]}{K_{\mathrm{m}} + [S]} \ , \tag{S6}$$

where $[P]$ is the concentration of the reaction product, and $[S]$ is the concentration of the substrate. V_{max} is the maximum kinesin velocity, and K_{m} (Michaelis constant) is the substrate concentration that provides half of V_{max}, as fitting parameters. V_{max} and K_{m} were obtained by fitting the Michaelis-Menten kinetics equation (S6) to plots for labeled and unlabeled ATP (Supplementary Table 1). The association rate constant k_{on} was calculated as $k_{\mathrm{on}} = \frac{k_{\mathrm{cat}}}{K_{\mathrm{m}}}$, where k_{cat} is the maximum reaction rate. The k_{cat} was calculated by dividing V_{max} by the step size of kinesin (8 nm), yielding 1.9×10^5 $\mathrm{M^{-1}s^{-1}}$ for labeled ATP and 4.8×10^5 $\mathrm{M^{-1}s^{-1}}$ for unlabeled ATP (Supplementary Table 1).

4. Supporting movie list

Supplementary Movie 1. Labeled ATP (50 nM) in TIRFM.
Supplementary Movie 2. Labeled ATP (250 nM) in TIRFM.

Supplementary Movie 3. Labeled ATP (1 μM) in LZMWs.
Supplementary Movie 4. Microtubule gliding in LZMWs.
Supplementary Movie 5. Simultaneous observation of GFP-fused kinesin, microtubules, and labeled ATP.
Supplementary Movie 6. Bleaching time of labeled ATP depending on the modulation frequency of the excitation light.

5. Reference

1. Levene, M. J.; Korlach, J.; Turner, S. W.; Foquet, M.; Craighead, H. G.; Webb, W. W. Zero-Mode Waveguides for Single-Molecule Analysis at High Concentrations. *Science* **2003**, *299*, 682–686.